Lanthanide-directed assembly of interfacial coordination architectures – from complex networks to functional nanosystems

David Écija,*[‡,⊥] José I. Urgel,[†,∥,⊥] Ari P. Seitsonen,[§] Willi Auwärter,[†] and Johannes V. Barth*[†]

[‡] *IMDEA Nanoscience, E-28049 Madrid, Spain*
[†] *Physik-Department E20, Technische Universität München, D-85748 Garching, Germany*
[§] *École Normale Supérieure, F-75005, Paris, France*

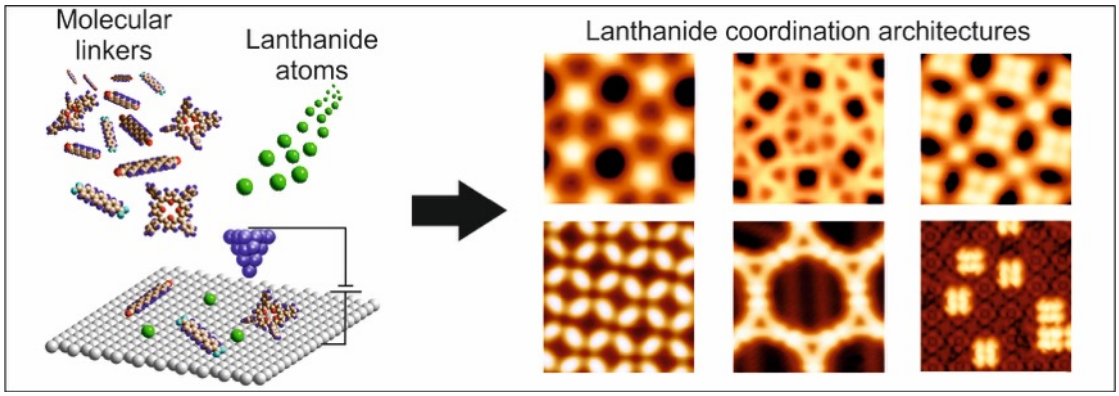

CONSPECTUS

Metallosupramolecular engineering on surfaces provides a powerful strategy towards low-dimensional coordination architectures with prospects for several application fields. To date most efforts concentrated on incorporating transition metals, and only recently we pioneered lanthanide-directed assembly. Coordination spheres and motifs with rare-earth elements generally display distinct properties and structural features. The size of the cations and shielding role of the 4f orbitals induces generally high coordination numbers, frequently entailing flexible coordination geometries. Following Pearson´s hard and soft acid-base theory, lanthanide cations

are hard Lewis acids, thus having strong affinity for nitrile, terpyridine and carboxylate donor moieties. The prevailing oxidation state is +3, although elements such as cerium and europium may adopt +4 and +2 values, respectively. The chemistry of rare-earth elements received widespread attention as they are key ingredients for established and emerging twenty-first century science and technology with importance for energy conversion, sensing, catalysis, magnetism, photonics, telecommunications, superconductivity, biomedicine and quantum engineering.

Herein we review recent advances towards designing interfacial supramolecular nano-architectures incorporating lanthanide centers. We apply controlled ultra-high vacuum conditions whereby atomistically clean substrates are prepared and exposed to ultrapure atomic or molecular beams of the chosen sublimabe constituents. We focus on direct, molecular-level investigations and *in situ* assembly protocols close to equilibrium conditions. Our scanning probe microscopy techniques provide atomistic insights regarding formation, stability and manipulability of metal-organic compounds and networks. In order to gain deeper insights into the experimental findings, a complementary computational analysis of bond characteristics and coordination motifs has been performed for several case studies. Exemplary elements under consideration include cerium, gadolinium, dysprosium, and europium. Using ditopic molecular linkers equipped with carbonitrile moieties, adaptive coordination spheres are unveiled, yielding vertices with two- to six-fold symmetry. The respective coordination nodes underly the expression of complex networks such as semi-regular Archimedean tessellations for cerium or gadolinium-directed assemblies and random-tiling quasicrystalline characteristics for europium. Tunability via constituent stoichiometry regulation is revealed for bimolecular arrangements embedding europium centers interacting with carbonitrile and terypyridine functional endgroups.

Carboxylate termini yield robust reticular networks based on a lateral coordination number of eight for either gadolinium or dysprosium complexation and feature a prevalent ionic nature of the coordination bond. Orthogonal insertion protocols gives rise to d-f reticular architectures exploiting macrocyclic tetradentate cobalt complexation and peripheral carbonitrile-gadolinium coordination, respectively. Furthermore, lanthanides may afford metalation of free-base tetrapyrrole species and allow for interfacial synthesis of sandwich compounds, thus providing prospects for columnar design of coordination architectures. Finally, performing manipulation experiments allow for both lateral displacement of single supramolecules, and molecular rotation of sandwich or other molecular units, paving avenues for controlled molecular motion on surfaces, whereby both translations and rotations are relevant for advancing molecular machinery components.

The presented achievements herald further advancements in metallo-supramolecular design on surfaces, with versatile nanosystems and architectures emanating from the flexible coordination spheres. The embedding and systematic rationalization of lanthanide centers in tailored interfacial environments is the key to establish relations between structure and physico-chemical characteristics towards generation of novel functionalities with application potential.

INTRODUCTION

The lanthanide (Ln) series comprises the fifteen metals from lanthanum (La) to lutetium (Lu); with the addition of yttrium (Y) and scandium (Sc) this constitutes the rare-earth elements. Similar with the actinides, the included *f*-block atoms feature an increasing filling of the inner *f*-electron shell, accounting for frequent chemical similarities and distinct spectroscopic characteristics. Nowadays, lanthanides are ubiquitous in technology where their unique physico-

chemical properties are exploited, underlying a multitude of applications in diverse sectors. They are essential constituents in, e.g., extraordinary strong permanent magnets, magnetocaloric alloy materials, high-temperature superconductors, and catalysts. Their photophysical properties find use in luminescent displays and lasers or sensors, energy up-converting nanomaterials and therapeutic agents, bio-probes, and medical diagnosis.[1] The rich coordination chemistry of lanthanides has been investigated with growing intensity since many years, originally often aiming at tailored optical features.[2] However, stunning developments also highlighted the potential for intricate coordination compounds and functional network architectures,[3,4] as well as molecular magnetism and spintronics,[5,6] together with prototype systems embedding lanthanides for quantum technology.[7,8]

Supramolecular chemistry provides powerful and versatile methodologies to design functional nanoarchitectures using well-defined surfaces as construction platforms. Following this strategy, *in vacuo* metal-directed assembly protocols have been explored towards the *in-situ* construction of novel interfacial metal-organic complexes and architectures, where mostly transition metals were employed.[9-13] Hereby, molecular linkers are designed *ex-professo* to incorporate coordinative functional groups, frequently inspired by established protocols involving other environments. The interfacial confinement frequently induces specific (e.g., planar) configurations of the linkers and upon coordination with metal centers, distinct coordination motifs are expressed. Importantly, the coordination spheres emanate under the simultaneous influence of the substrate atomic lattice and the ligands, which effect often affords coordinatively unsaturated apical sites[13] able to interact with adducts. The supramolecular nanosystems typically evolve at near-equilibrium conditions whence kinetic limitations are usually irrelevant.[9,13] In addition, a delicate interplay between enthalpic and entropic contributions directs the system formation, in which

typically the loss of entropy is compensated with the enthalpic contributions by maximizing the number of supramolecular interactions. Within these considerations, the subtle balance between metal-organic, molecule-substrate and molecule-molecule interactions is decisive for the distinct coordination complexes or network topologies achieved. Such metal-organic systems are commonly termed based on the number of coordination (2-fold, 3-fold, 4-fold, 5-fold or 6-fold) or the specific geometry of the network topology. Hereby, most of reported nanostructures are 0D, 1D or 2D systems, while new efforts will focus on the design of 3D architectures exploiting the potential columnar growth of specific metal-ligand interactions.

The surfaces of elemental lanthanides and thin films, their oxides and alloys have been extensively investigated since the 1970s to the current era, but atomistic studies addressing Ln species at interfaces remained scarce.[14,15] However, recent breakthroughs reveal intriguing magnetic behaviour of single Ln atoms positioned at well-defined surfaces *in vacuo*.[16,17] Moreover, considerable efforts were made regarding interfacial confinement and control of lanthanide-based single-molecule magnets towards their integration in nanoscale device elements.[18-20]

Herein we review our systematic efforts to develop *in situ* protocols for lanthanide-directed assembly at well-defined surfaces, whose construction principles along with the presently known library of coordination motifs are summarized in scheme 1, and identify the associated prospects for designing functional nanoscale systems and architectures. Emphasis is put on direct insights by scanning tunneling microscopy (STM) using low-index coinage metal substrates. frequently complemented by computational modeling using density functional theory (DFT).

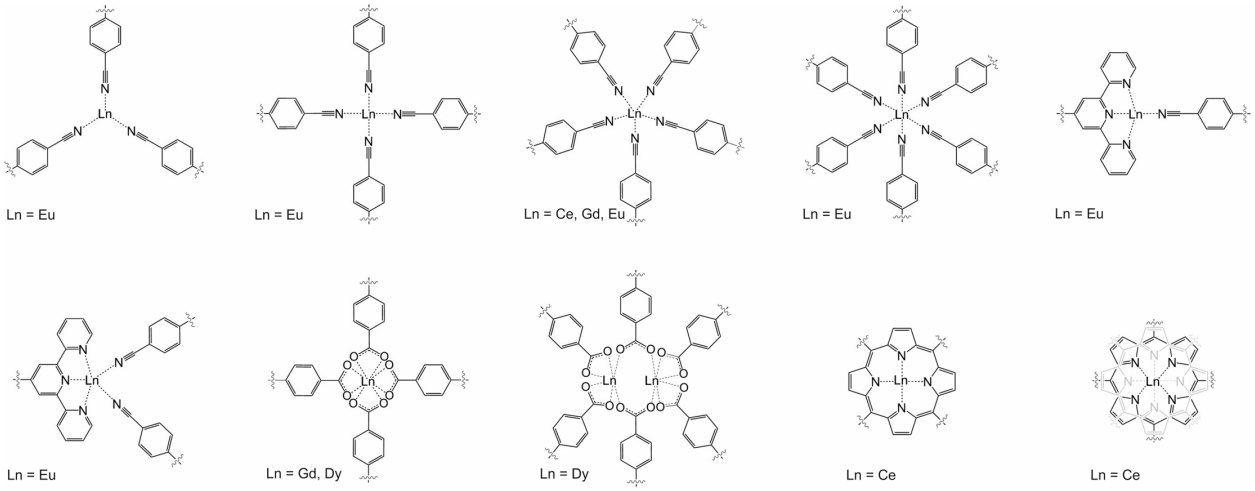

Scheme 1. Protocol for Ln-based interfacial metallosupramolecular design and established library of coordination motifs.

NITROGEN-DONOR LIGANDS

Carbonitrile moities proved particularly successful in recognizing transition metal atoms on the smooth fcc(111) surfaces of Ag or Cu, giving rise to metal-organic architectures where three-fold and four-fold coordinations nodes prevail.[21,22] Simultaneously, carbonitrile terminal groups were used for the synthesis of lanthanide-organic compounds in solution targeting luminescent metal-organic frameworks[23] or molecular magnetic materials.[24,25] Inspired by these promising results in the last lustrum, we realized lanthanide-directed architectures on coinage metals.[26-30] The prevailing expression of five-fold and six-fold coordination entails complex organizations, including semi-regular Archimedean tiling tessellations[26,27,30] and random tiling quasicrystals.[30]

Notably, ditopic linear carbonitrile linkers with poly(p-phenylene backbones) (see the exemplary quarterphenylene-dicarbonitrile species named QDC in Figure 1a) were employed on Ag(111). Their assembly directed by cerium (Ce) or gadolinium (Gd) centers at room temperature renders five-fold CN···Ln coordination vertices, and by precise stoichiometric control provides: i)

individual pentameric supramolecules; ii) a hexagonal lattice from dodecameric subunits, additionally stabilized by lateral CN···phenyl interactions, and iii) fully reticulated 2D metal-organic network (cf. left, central and right panel of Figure 1b, respectively). The latter case represents a snub-square tiling based on triangles and squares, with each center sharing three triangles and two squares according to a 3.3.4.3.4 pattern. Furthermore, the related elongated-triangle tiling with a 3.3.3.4.4 scheme can evolve,[26,27] and similar results were obtained employing a shorter linker and Ce.[26] Importantly, the coordination spheres, with projected CN···Ln bond distances from 2.2 ± 0.5 to 2.8 ± 0.5 Å, are flexible with opening angles between adjacent molecules ranging from 60 ± 5 to 85 ±5°.

In 3D compounds, Ce^{III}, Gd^{III} and Eu^{III} ionic radii are 103, 93.8 and 94.7 pm, respectively, whereas Eu^{II} features a value of 131 pm, signaling prospects for increased flexibility. Indeed, the stochiometrically controlled Eu-directed assembly of QDC on Ag(111) affords both regular square lattices and snub-square Archimedean tilings (cf. Figure 1c), reflecting 4-fold and 5-fold coordinative schemes. Remarkably, implementing a similar protocol on Au(111)[30] yields a variety of networks for changing Eu:QDC stoichiometric ratios (cf. Figure 1d). Surprisingly, three- to six-fold lateral coordination motifs now account for random string networks, reticular four-fold assemblies, complex tiling schemes, and hexagonal lattices. The high degree of adaptability could reflect reduced adsorbate-substrate interactions and size effects of Eu cations, in conjunction with the intrinsically ionic nature of lanthanide coordination.

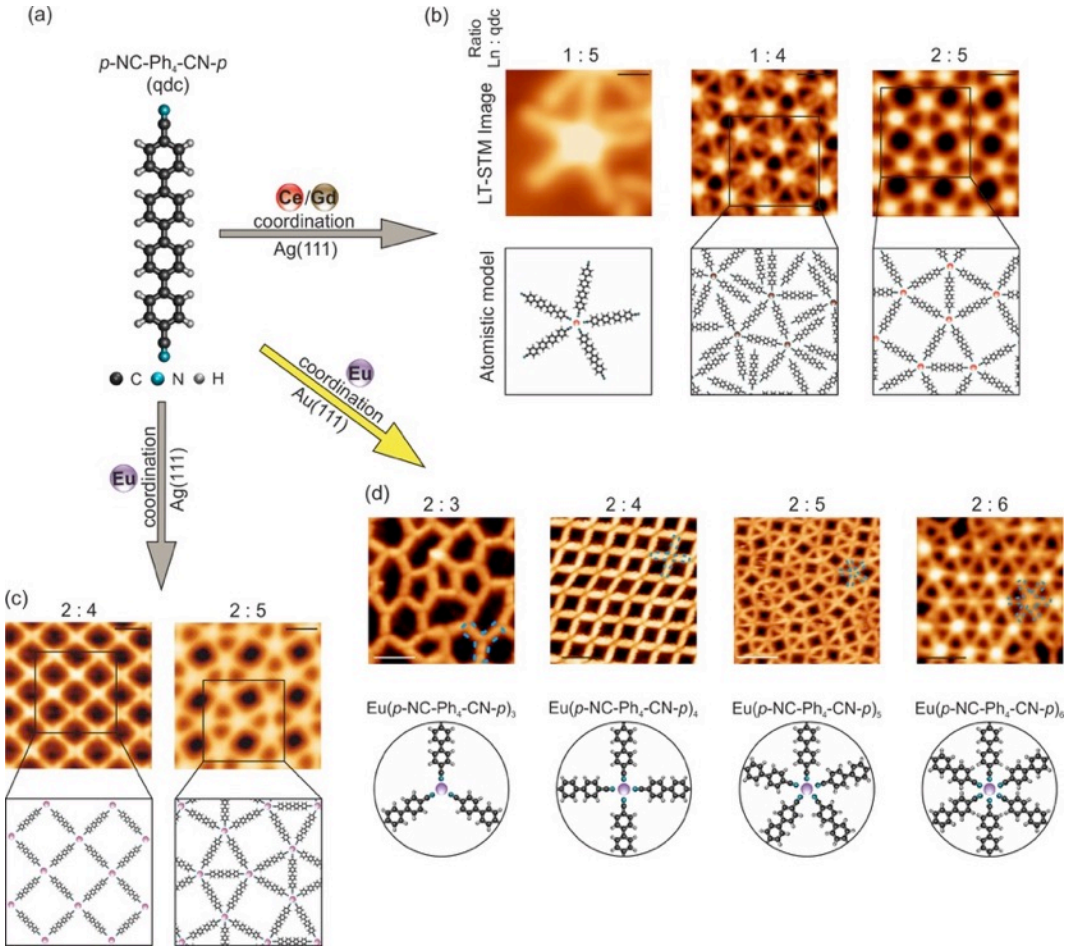

Figure 1. Lanthanide-carbonitrile coordination networks on surfaces. a) Ball-and-stick model of a quaterphenylene-dicarbonitrile species (QDC: black, C; light blue, N; white, H). b) QDC-Ce/Gd coordination on Ag(111). STM images and corresponding atomistic models for different Ln : QDC ratios with five-fold coordination motifs (measured at 6 K, ratios of 1:5/1:4/2:5; scale bars 1/2/2 nm, respectively). Adapted with permission from ref. 27. Copyright 2014 American Chemical Society. c) QDC-Eu networks on Ag(111). STM images measured at 300 K and corresponding atomistic models for indicated Ln:QDC ratios (scale bar 2 nm). d) QDC-Eu coordination on Au(111). STM survey of different coordination networks upon variation of the Eu : linker stoichiometry, with corresponding atomistic models (measured at 300 K, scale bar 5 nm). Adapted with permission from ref. 30. Copyright 2016 Nature Publishing Group.

The most intriguing phase is the fully reticulated layer depicted in Figure 2a (~ 2:5 Eu to QDC ratio) with Eu centers surrounded by four, five or six linkers. Eu-NC bonds have a projected length of 2.6 Å, similar with Ce- and Gd-based nodes. The combination of square and triangle motifs reflects dodecagonal quasicrystalline characteristics. Accordingly, the encountered tessellation of the plane by triangle and squares lacks translational symmetry, though distinct motifs can be identified (cf. Figure 2b): 3^6 hexagonal, five-vertex $3^2.4.3.4$ snub square, and $3^3.4^2$ elongated triangle, with respective proportions of 6%, 62%, 13% counted in a set of >400 nodes.

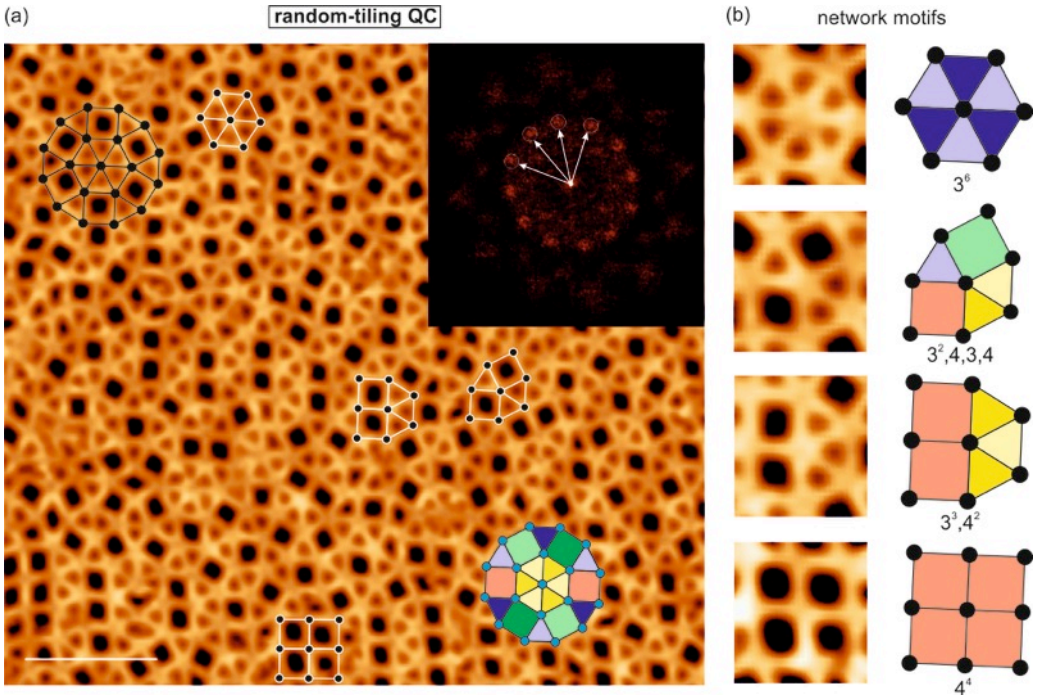

Figure 2. Metal-organic square-triangle random-tiling network on Au(111) with dodecagonal symmetry. a) STM topograph with characteristic structure elements indicated; linker : Eu stoichiometric ratio ~ 2 : 5.1; inset shows 12-fold symmetric 2D-FFT (STM measurement at 300 K, 10 nm scale bar. b) Motifs and models showing six-fold (3^6), five-fold ($3^2.4.3.4$ and $3^3.4^2$) and four-fold coordination (4^4) , and different orientations of squares and triangles. Adapted with permission from ref. 30. Copyright 2016 Nature Publishing Group.

Furthermore a fraction of nodes could not be conclusively assigned, and a non-negligible number of 4^4 four-fold nodes exists (2%). The latter represent a characteristic feature of random

square-triangle tessellations, originally hypothesized in theoretical considerations,[31-33] whereby the triangle-to-square number ratio is 2.31,[31] close to the value 2.36±0.01 determined for our findings. There are three distinct orientations for the embedded squares and four for the triangles, respectively, i.e. in total 12 linkers orientations are possible. Corroborating the above assignment of quasicrystalline order, the Fast-Fourier transform of the STM topography exhibits a 12-fold rotational symmetry (cf. inset Figure 2a). Moreover, both a statistical evaluation of STM data[30] and mathematical analysis[34] indicate preferential orientations of tiling units, presumably reflecting the influence of the Au(111) reconstruction. Interestingly, such a random tiling quasicrystal is suggested to appeared as a subtle balance between entropic and enthalpic contributions, whereby entropic forces maximize randomness by expressing a random tessellation of squares and triangles, whereas enthalpic contributions arise from adlayer/substrate and lateral metal-ligand interactions.

The flexibility of the Eu coordination sphere was also exploited to fine-tune Eu-directed metallosupramolecular binary networks by regulating ligand stoichiometry.[29] The codeposition of QDC and a ditopic terpyridyl linker (cf. Figure 3a) on the Au(111) substrate held at room temperature followed by evaporation of Eu yields terpyridine-Eu-carbonitrile links. For a QDC:terpyridyl stoichiometric ratio of 0.7, the ensuing four-fold coordination stabilizes one-dimensional binary metal-organic chains (cf. Figure 3b). Increasing the ratio to 0.9 gives rise to a mixture of chain segments and three-way junctions with five-fold coordination motifs (cf. Figure 3c). Finally, for a ratio of 1.8 two porous reticulated networks occur: a honeycomb and a fishing-net superlattice (cf. Figure 3d,e), both comprising five-fold metal-organic coordination nodes while reflecting different packing densities.

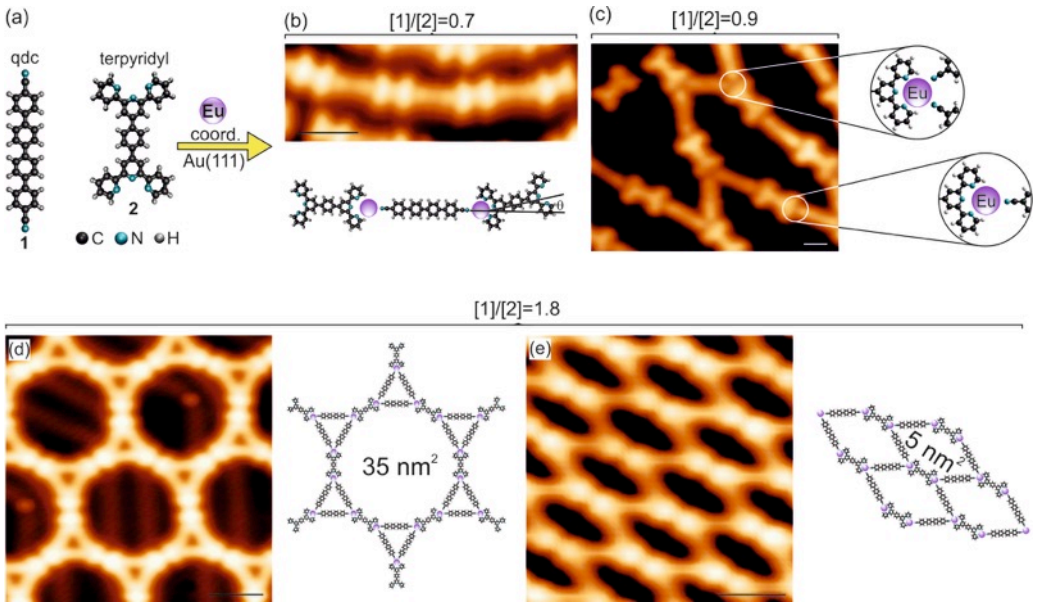

Figure 3. Bimolecular europium-directed metallo-supramolecular chains and networks on Au(111). a) Ball-and-stick atomistic model of QDC (1) and terpyridyl (2) linkers (black, C; light blue, N; white, H). b) STM image model of metal–organic chains formed at a stoichiometric ratio of [1]/[2] = 0.7 (measured at 5 K, scale bar 1 nm). c) Four-fold and five-fold coordination motifs coexisting for stoichiometric ratio [1]/ [2] = 0.9 (measured at 77 K, scale bar 1 nm). d-e) Two-dimensional reticulated networks with different packing density formed for [1]/[2] = 1.8 (measured at 77 K, scale bar 3 nm). Adapted with permission from ref. 29. Copyright 2016 Royal Society of Chemistry.

Recently, assembly protocols that exploit orthogonal coordination interactions to tackle the design of d-f metallo-supramolecular architectures were developed.[35] Such hybrid systems combining lanthanides and transition-metal centers synergetically interacting in specific environments are targeted for functionalities that cannot be obtained from separate constituents, e.g. relevant for light-emitting devices.[36] Also in magnetism and spintronics magnetic exchange coupling between the 3d and 4f elements can be favorable.[37,38]

To realize a prototype d-f surface-confined metallo-supramolecular nanoarchitecture, we employed the tetradentate cyanobiphenyl-substituted free-base porphyrin 2H-TPCN, cf. Figure 4a,b).[35] Codeposition of 2H-TPCN and Gd on Ag(111) held at 300 K gives rise to a 2-D reticulated metal-organic network based on four-fold CN···Gd coordinative links (projected bond-distance of 2.7 ± 0.5 Å), whereby the macrocyclic pockets remain unaffected (cf. Figure 4c). By contrast, deposition of cobalt (Co) on a submonolayer coverage of 2H-TPCN entails selective metalation of tetrapyrrole cores, whereas the formation of CN···Co coordinative links is inhibited. Accordingly, we implemented a three-step scheme: i) deposition of free-base TPCN species, ii) Gd-directed assembly of Gd-2H-TPCN networks, and iii) exposure to a Co atomic beam affording heterometallic networks (cf. Figure 4b-d). Herein the TPCN species are exclusively engaged laterally in four-fold CN···Gd coordinative interactions. Furthermore, no clustering of Co adatoms interferes and an appreciable fraction of tetrapyrrolic macrocycles undergoes selective Co-metalation, without affecting the regularity of the lanthanide-directed coordination network.

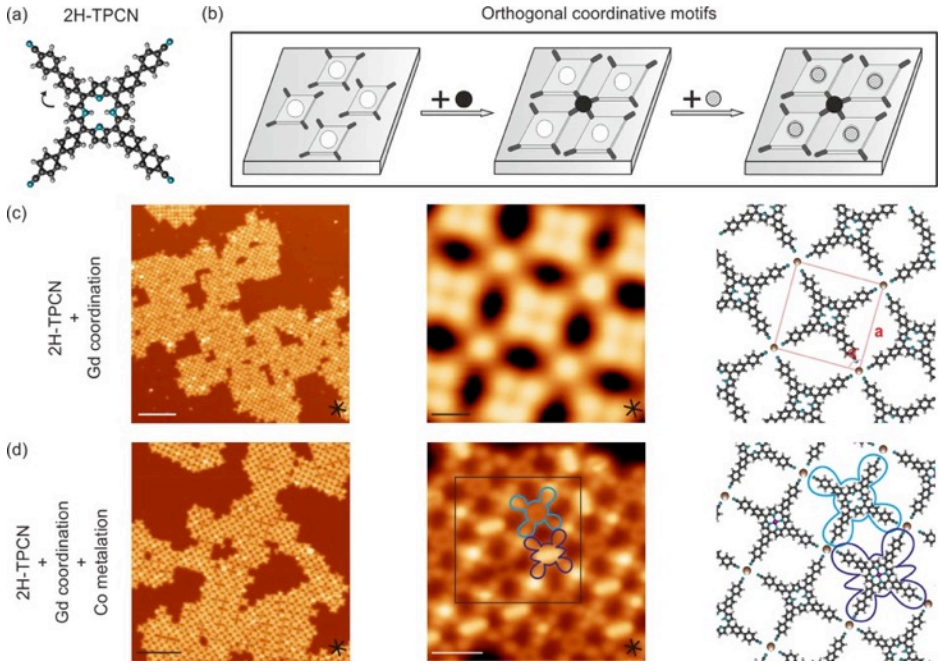

Figure 4. Orthogonal insertion of lanthanide and transition metal centers. a) Ball-and-stick model of the 2H-TPCN building block (black, C; light blue, N; white, H). b) Orthogonal coordination motif benefiting from the cyano-substituents and intramolecular macrocycles. Lanthanide (transition metal) atoms depicted as black (grey) spheres. c) Four-fold Gd-carbonitrile coordination yields an open metal-organic network (left/right: overview/close-up image, scale bar 20/1 nm). Ball-and-stick atomistic model shows the square unit cell, with vector $\boldsymbol{a}$ and angle α. d) Heterobimetallic Gd-Co network following selective macrocycle metalation by Co (left/right: overview/close-up image recorded at V_s = 1 / -1 V, I_t = 100 / 75 pA, scale bar 10 / 2 nm; note that positive bias is used for grid-like assembly inspection, at negative bias the characteristic rod-like appearance of metalated macrocylces appears). Data measured at 6 K employing a Ag(111) substrate. Adapted with permission from reference 35. Copyright 2015 Wiley.

IN-SITU SYNTHESIS OF LANTHANIDE TETRAPYRROLE COMPLEXES

Lanthanides can be sandwiched between macrocyclic ligands, resulting in 3-D complexes. Specifically, double- and multideckers of lanthanide-tetrapyrroles attract considerable interest due to their distinct electronic, magnetic[5,6,8,39-41] and nanomechanical properties (*vide infra*). However, first attempts to realize Ce double-deckers with a mixture of tetraphenylporphyrin (2H-TPP) and CoTPP on Ag(111) afforded only half-sandwich lanthanide species,[42] subsequently associated with Ln-decoration of CoTPP,[43,44] similar to Fe uptake reported elsewhere.[45]

The recent study also identified sitting atop (SAT) complexes and their transformation to Ce-TPP upon thermal annealing or local tunneling voltage pulses (cf. Figure 5b-g),[43,44] whereby the Ce center is displaced out of the macrocycle plane.[42] In parallel an alternative co-deposition approach using a supersonic 2H-TPP beam achieved films of erbium-TPP complexes on a SiO/Si(100) support.[46]

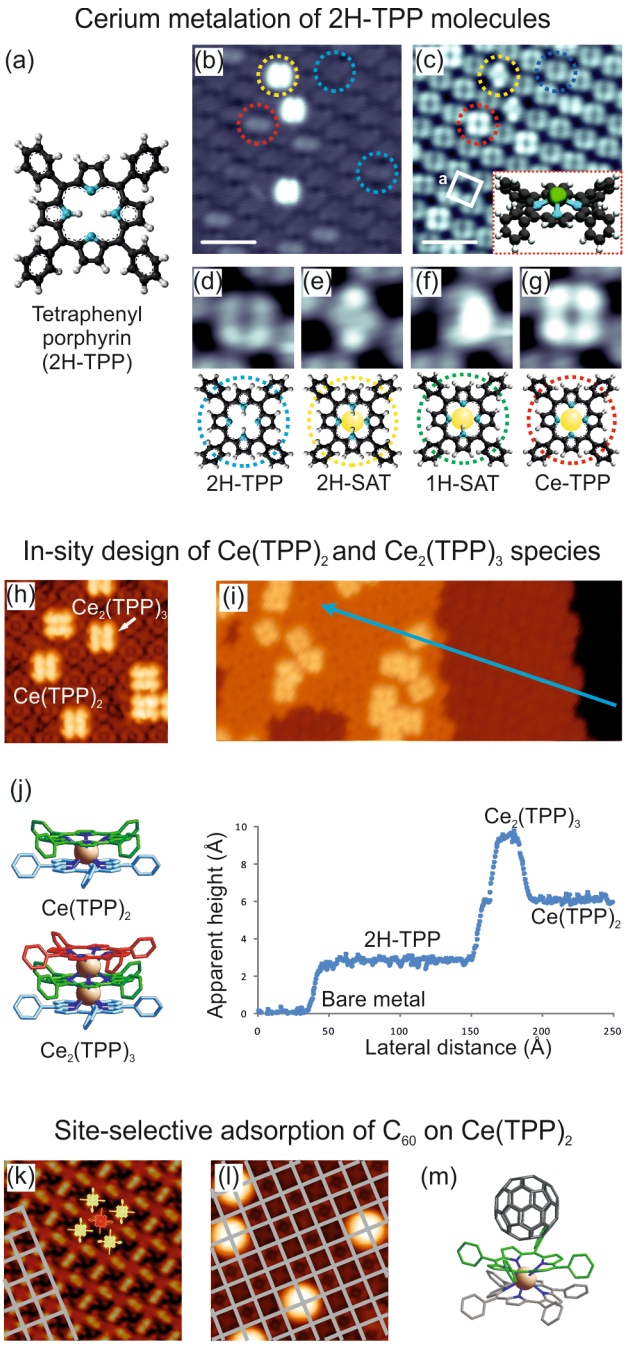

Figure 5. ***In-situ*** **assembly and lanthanide metalation pathways with tetrapyrroles on Ag(111).** a) 2H-TPP building block. b-g) 2H-TPP arrays decorated with Ce centers and STM-induced transformations. h-i) *In-situ* design and identification of Ce-TPP double- and triple-decker species embedded in a 2H-TPP array. Adapted with permission from reference 47. Copyright 2011 Wiley. k-m) Selective uptake of fullerenes by top macrocycles of a regular Ce-$(TPP)_2$ array. Adapted with permission from ref. 48. Copyright 2012 American Chemical Society.

In subsequent work, a multilayer metalation / desorption protocol was developed, yielding true $Ce(TPP)_2$ and $Ce_2(TPP)_3$ complexes embedded in 2H-TPP arrays on Ag(111) (cf Figure 5h-j).[47] This implies an initial 2H-TPP multilayer deposition, subsequent exposure to an atomic beam of Ce, and an annealing step at 500 K, inducing both metalation and desorption of unreacted multilayer components. STM inspection clearly reveals the coexistence of $Ce(TPP)_2$ and $Ce_2(TPP)_3$ species featuring a characteristic apparent height of 6 and 9.4 Å, respectively (cf. Figure 5i). The complexes are preferentially arranged in dense-packed islands, where the top ligand in $Ce(TPP)_2$ is rotated by 45±5° relative to the bottom one, adapting a bowl-like conformation.[48]

Finally, $Ce(TPP)_2$ arrays were successfully employed as template for site-selective adsorption of fullerenes. Individual C_{60} molecules with distinct orientation center above the deformed TPP top-ligands, thus forming van der Waals stabilized dyads that can be employed as molecular switches or prospective donor-acceptor pairs with photophysical response (cf. Figure 5k-m).[48]

COMPUTATIONAL MODELLING

It is beneficial to perform calculations for conclusive interpretation and a deeper understanding of experimental findings. Thus far DFT modeling efforts mainly concentrated on the properties of the final structures. It must be appreciated that the computational efforts are demanding and require simultaneously an adequate description of the lanthanide, molecular and surface electronic configuration, as well as the entire scope of binding contributions, ranging from chemical bond formation to electrostatic and van der Waals interactions.

Notably several of the bonding schemes described above were addressed (cf. next section for carboxylate linkers). A calculation for five-fold Ce-CN coordination on Ag(111) is depicted in

Figure 6a.[26,27] The derived atomic geometry agrees well with the experimental characteristics and important further details are disclosed. Notably the phenylene backbone is nearly planarized due to van der Waals interaction with the substrate, as opposed to the typical gas phase phenylene rotation from the steric intereference of adjacent rings. Ce-N distances range from 2.56 to 2.59 Å in the individual supramolecules, and from 2.52 to 2.60 Å in the dodecameric network.[27] The respective angles between the ligands range from 67 to 80° and from 61 to 81° for the static situation (temperature effects could increase the variation). The carbonitrile-lanthanide interaction entails an electron density reorganisation, reproduced in Figure 6a for a single pentameric unit, including a slight charge transfer and polarisation of the ligands.

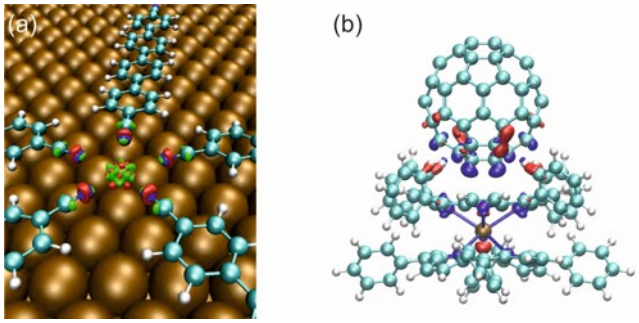

Figure 6. Modeling structural features and charge rearrangement in lanthanide-directed assemblies. (a) Pentameric supramolecule with five-fold coordination of Ce by carbonitrile linkers on Ag(111). The average distance between the Ce ion and N atoms is 2.58 Å. (b) C_{60}-Ce(TPP)$_2$ complex following attachment of C_{60} on the double decker molecule. Red indicates gain of electrons and blue electron depletion. Adapted with permission from ref. 48. Copyright 2012 American Chemical Society.

Early modeling efforts of Ce-porphyrin species addressed isolated half-sandwich compounds as first step. Insertion of Ce into H_2-TPP requires an evaluation of the Ce atom energetics, the lanthanide connection to H_2-TPP yielding H_2-TPP+Ce, and the final product with dihydrogen abstracted. Indeed, Ce-TPP is energetically more stable by 0.8 eV over the H_2-TPP+Ce complex,

indicating that the former may form on the substrate. Moreover, for Ce-TPP the lanthanide center is displaced by 1 Å from the macrocycle plane with a Ce-N bond length of 2.3 Å.

We also modeled the Ce-$(TPP)_2$ double-deckers and their selective decoration by C_{60}. In Ce-$(TPP)_2$ the porphyrins are bent away from each other for steric reasons, whence the molecules are rotated into a propeller-like arrangement. Moreover, the bowl-like conformation of the upper porphyrin ligand provides a suitable adsorption site for C_{60} by increasing the area of close proximity in the complex, thus supporting molecular recognition. Although the electron density polarises following C_{60} attachment (cf. Figure 6b), the attraction between the fullerene and the macrocycle is dominated by van der Waals interactions. In the orientation where 6:6 bonds point towards both the vacuum and TPP side, the binding energy is 1.16 eV, which value is lowered to 1.09 eV for apex atoms as extrema. The related magnitude of the potential energy surface corrugation is large enough for separating metastable configurations, but yet allows that different configurations can be populated.

CARBOXYLATE LIGANDS

Carboxylate linkers were extensively and successfully used for designing functional 3-D metal-organic frameworks, including lanthanide-based constructs.[49,50] For establishing structure-property-functionality relationships with relevance for both 2-D and 3-D architectures, it is helpful to realize and examine interfacial systems. Inspired by pioneering studies of carboxylate moities and transition metal atoms on coinage metals,[9,10,51] we focused on linear and tripod carboxylate linkers with polyphenyl backbones (cf. Figure 7).

Upon moderate annealing on Cu(111), adsorbed TDA species (cf. Figure 7a) readily deprotonate. Subsequent co-deposition of Gd induces fully reticulated metal-organic networks, with a square unit cell (side length 19.5 ± 0.7 Å). Molecules are imaged as rod-like protrusions and lanthanide

centers as voids or faint features, depending on tip conditions. A closer inspection reveals that four carboxylate endgroups point straight to Gd centers with a projected distance of 2.6 ± 0.7 Å (cf. Figure 7b,c). Corresponding DFT simulation support eight-fold Gd···O lateral coordination whereby the carboxylate moieties are rotated for steric reasons (using for simplicity the smaller linker analogue TPA, benzene-1,4-dicarboxylic acid). Moreover, the charge-density displacement field of the Gd-TPA_4 node (cf. Figure 7d), i.e. the difference between the electronic densities of the interacting system and those of its non-interacting components, was determined. It reveals electronic depletion zones around the Gd center, reflecting metal-ligand interactions with strong ionic contribution. This picture is confirmed by comparative X-ray photoelectron spectroscopy of non-coordinated and Gd-coordinated TPA species, which shows that the oxygen 1S peak only shifts by 0.1 eV upon Gd-carboxylate bonding (Gd in +3 oxidation state). Upon substrate temperature variation from 77 to 360 K the networks and island borders are unaffected, thus highlighting the robustness of the grid structure.

Further insights were gained with dysprosium (Dy) that affords analogous assemblies as those directed by Gd, i.e. based on 8-fold vertexes. Both topographic STM-appearance and X-ray spectroscopy concur, reflecting again predominantly ionic interactions (cf. Figure 7e). However, further annealing to 450 K generates a modified porous layer, rationalized as a quasi-hexagonal network presenting dinuclear Dy centers (cf. Figure 7f) – which signals prospects for multi-nuclear lanthanide-directed surface-confined nanostructures. Next, we explored the tunability of the cavity size by the linker length. Employing pyrene-2,7-dicarboxylic acid and TPA and similar preparation conditions afforded indeed isostructural reticular and mononuclear metal-organic nanomeshes based on eight-fold Dy···O interactions, whose internodal distances were 11.8 ± 0.5 Å for TPA and 15.4 ± 0.5 Å for PDA vs. 20.5 ± 0.5 Å for TDA, respectively.

However, the expression of dinuclear nodes did not occur for TPA and PDA species, which might reflect substrate registry effects disfavoring certain arrrangements. Finally, with the tripod linker BTB, cf. Figure 7g) fully reticulated metal-organic random network can be generated, again displaying 8-fold mononuclear Gd-carboxylate nodes (cf. Figure 7h). It is important to note that to date no indications exist that lanthanide-carboxylate coordination nodes can be controlled by constituent stoichiometry.

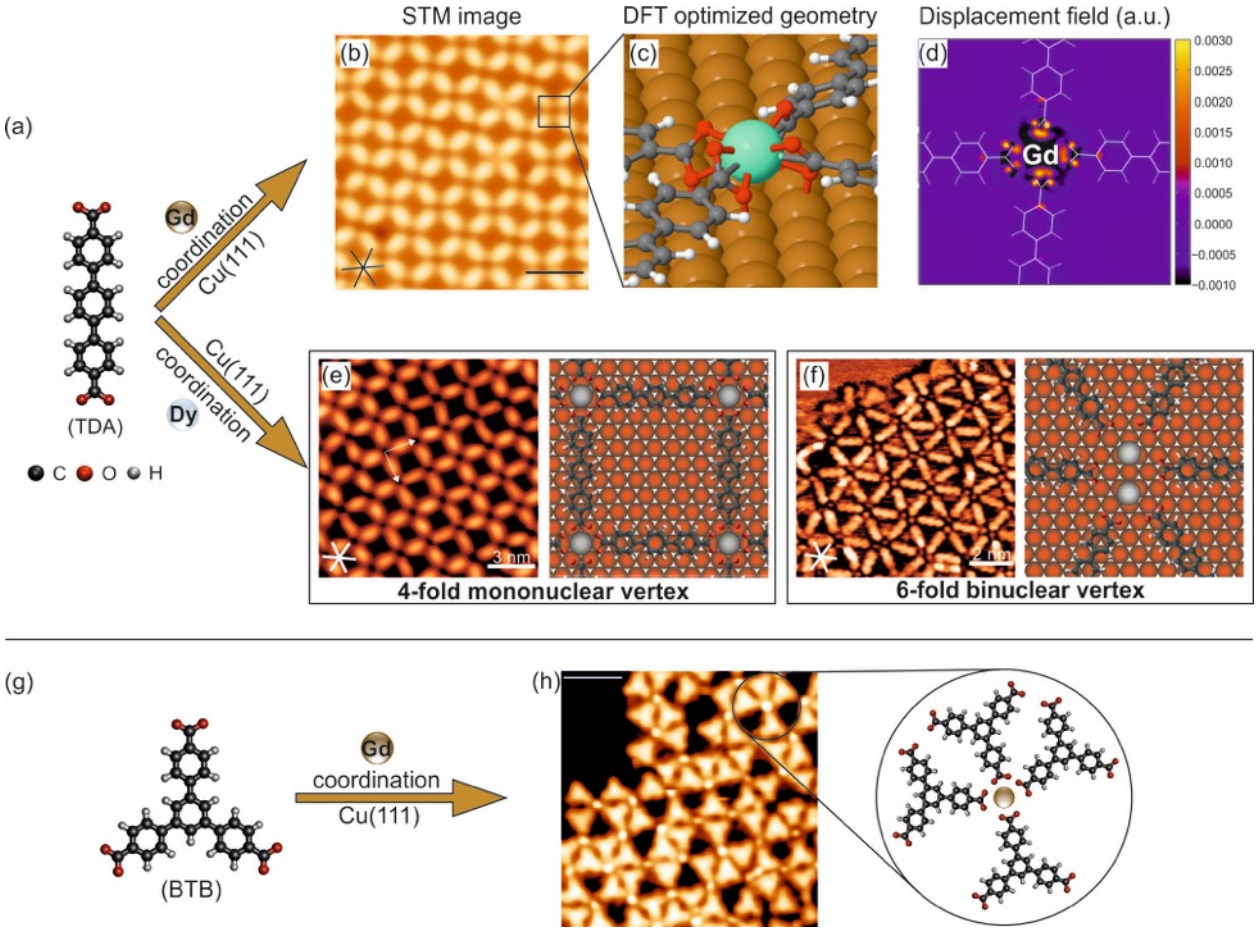

Figure 7. Lanthanide-carboxylate metallo-supramolecular networks on Cu(111). a) Ball-and-stick model of TDA linker. b-d) Gd-carboxylate grid with square unit cell and 8-fold lateral coordination. b) STM image measured at 6 K, 3 nm scale bar; c,d) DFT optimized geometry of the coordination node with rotated carboxylate groups and corresponding charge density displacement field (structure model is superimposed; negative values (violet, black) represent charge depletion, indicating ionic character of Gd, positive values (yellow, orange, red) reveal charge

transfer to carboxylate moieties. Adapted with permission from ref. 52. Copyright 2015 Wiley. e) Dy-carboxylate network with four-fold mononuclear coordination and corresponding DFT optimized geometry (3nm scale bar in STM image at left). f) Pseudohexagonal lattice induced by thermal annealing (420 K) with Dy : TDA six-fold binuclear coordination supported by DFT modeling (2 nm scale bar in STM image at left). Adapted with permission from ref. 53. Copyright 2016 Royal Society of Chemistry. g) Ball-and-stick model of the BTB linker. h) Lanthanide-directed Gd : BTB network. STM data measured at 6 K (3nm scale bar); the corresponding ball-and-stick model shows the four-fold coordination node.

DIRECT MANIPULATION OF LANTHANIDE-COORDINATED SUPRAMOLECULES

Taking advantage of the STM capabilities for atomic and molecular manipulation, selected lanthanide-based nanosystems were probed. Firstly, by positioning the STM tip above the vertex of gadolinium-coordinated supramolecules and adjusting the tip-metal distance to reach the attractive regime, the pentamers were laterally displaced with high reliability (cf. Figure 8a-f). In addition the tip was used to perform molecular surgery, extracting and replacing individual linkers to realize tetrameric, pentameric, nonameric and dodecameric metal-organic arrangements.[54] Secondly, lanthanide sandwiched double- and triple-deckers were addressed. Either by voltage pulses or by tip-induced lateral manipulation, molecular rotation of the top moiety could be achieved on phthalocyanine (cf. Figure 8g-i)[20] and porphyrin[47] species (cf. Figure 8j). Remarkably, voltage pulses in $TbPc_2$ complexes allowed the switching of a Kondo resonance attributed to an unpaired spin in a molecular orbital.[40] Finally, it was directly shown, that the fullerene-$CeTPP_2$ system described above provides a three-level molecular switching device where distinct cage orientations can be adjusted by the STM tip (cf. Figure 8k-m).[48]

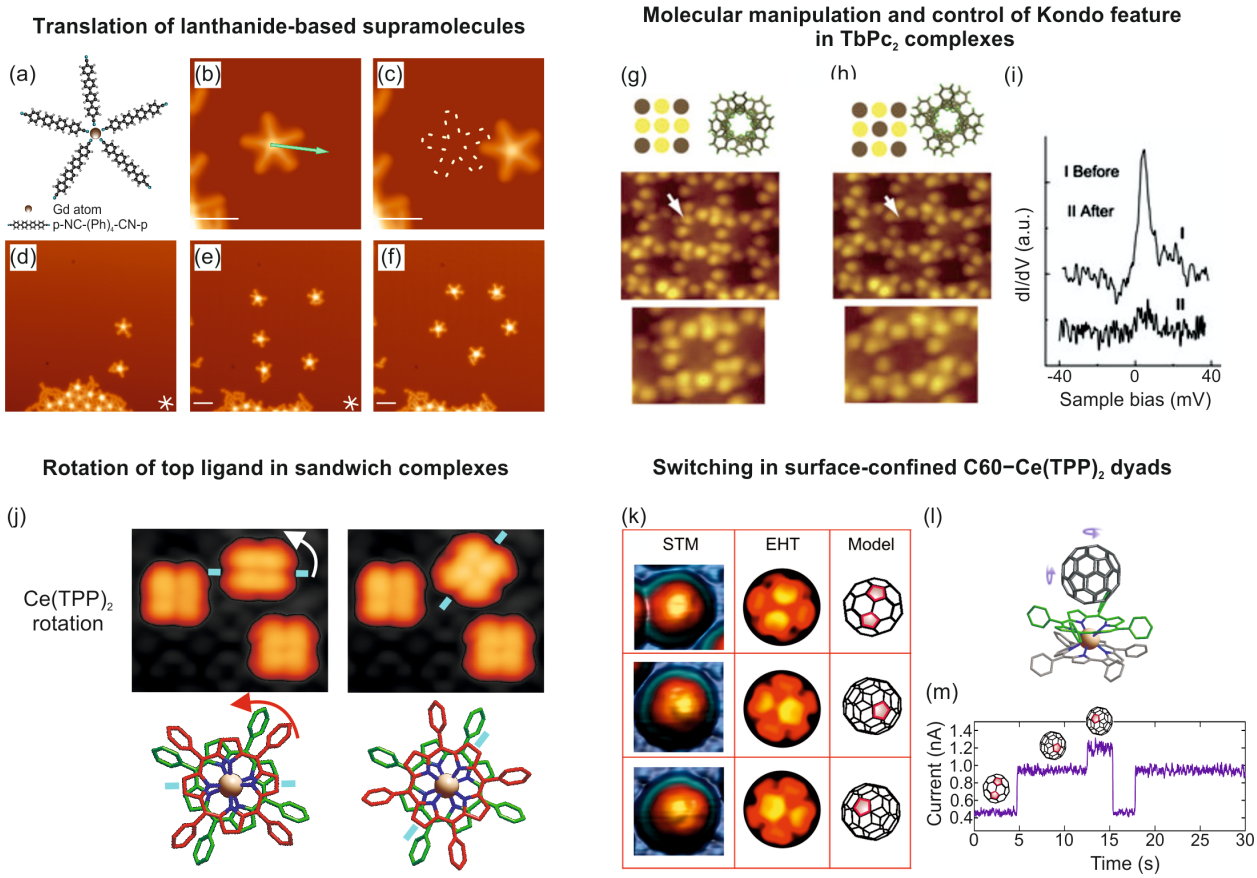

Figure 8. Translation and rotation of lanthanide-coordinated supramolecules. a-f) Translation of Gd-based supramolecules on the Ag(111) surface. a) Ball-and-stick atomistic model of a Gd-based pentameric unit. b-f) High-resolution STM images illustrating the lateral manipulation of pentameric units in constant current mode. Adapted with permission from ref. 54. Copyright 2014 American Chemical Society. g-i) Molecular rotation and switching of Kondo resonance on $TbPc_2$. Adapted with permission from ref. 20. Copyright 2014 Elsevier. j) Molecular rotation of top porphyrin ligand in $Ce(TPP)_2$ and $Ce_2(TPP)_3$ complexes. k-m) Geometric and electronic switching in C_{60}-$Ce(TPP)_2$ dyads. Adapted with permission from ref. 48. Copyright 2012 American Chemical Society.

FUTURE PERSPECTIVES

The survey of results exemplifies the abundant potentialities of lanthanides for directing the formation of complex metallo-supramolecular nanosystems on surfaces. Intricate compounds, tessellations and networks were introduced. Simultaneously, by using porphyrinoid tectons

prospects for molecular machinery, orthogonal insertion and three-dimensional architectures appear. These findings herald multiple promises for advanced interfacial metallo-supramolecular design employing lanthanide centers, targeting intriguing phenomena for both structural organization and functionality. Based on further exquisite molecular-level insights, sophisticated spectroscopy methods and computational modeling, the development of principles for rational design is envisioned.

Current perspectives include the creation of binary and ternary multi-metal constructs to exploit synergetic interactions of constituents, the embedding of multinuclear centers, the employment of additional linking groups, the realization of organo-lanthanide architectures, and the broad use of macrocyclic species. In addition, inspired by 3-D lanthanide-based metal-organic compounds and networks achieved in bulk chemistry exhibiting motifs with 6- to 12-fold, future efforts will focus on interfacial metallosupramolecular design with high coordination numbers and capabilities for three-dimensional growth.

Moreover, the fabrication of Ln-based nanostructures or hybrid systems on unconventional surfaces such as insulators, 2D-sheet or topological materials is expected, targeting to exploit the electroluminescent or magnetic properties of decoupled lanthanides, while adding fascinating routes in exotic supports by doping, spin-orbit coupling or proximity-induced ferromagnetism.

By meeting these appealing challenges and capturing the rich opportunities provided in the field, significant advances for physics, chemistry and materials science of the twenty-first century seem assured, providing substantial prospects for both fundamental research and technology.

AUTHOR INFORMATION

Corresponding Authors

* david.ecija@imdea.org; jvb@tum.de

Present Address

⁄⁄ pres. address: EMPA, Swiss Federal Laboratories for Materials Science and Technology, 8600 Dübendorf, Switzerland

Author Contributions

+ D.E. and J.I.U contributed equally.

BIOGRAPHICAL INFORMATION

David Écija is a 'Ramón y Cajal' fellow and leader of the 'Molecular Nanoarchitectonics at Surfaces' group at IMDEA Nanoscience, Madrid. His present research interests include chemical physics, molecular nanoscience and catalysis on surfaces. He holds a PhD in physics from Universidad Autónoma de Madrid. He was a Marie Curie fellow and researcher at TU München, before joining IMDEA Nanoscience in 2014.

José I. Urgel holds a MSc in chemistry from Universidad de Alcalá and a MSc in material engineering from Universidad Complutense de Madrid. In 2016, he completed his PhD studies at TU München for a thesis focused on lanthanide-directed architectures. Actually, he is a Postdoctoral Researcher at the Swiss Federal Laboratories for Material Science and Technology (Empa) where his main research interest is dedicated to on-surface chemistry.

Ari Paavo Seitsonen obtained his MSc at the Helsinki University of Technology (now part of Aalto University) in 1993 and his PhD at Fritz-Haber-Institut der Max-Planck-Gesellschaft in 2000. He was post-doctoral fellow at Università La Sapienza in Rome, Max-Planck-Institut für

Plasmaphysik in Garching-bei-München, Max-Planck-Institut für Festkörperforschung in Stuttgart, Centro Svizzero di Calcolo Scientifico of Eidgenössische Technische Hochschule Zürich in Manno (TI) and Universität Zürich. In 2005 he obtained a position at Centre National de la Recherche Scientifique in Paris as ingénieur de recherche. His research interests include properties of liquids and solvation, and properties of surfaces using computational methods.

Willi Auwärter completed his PhD at the University of Zurich in 2003. Subsequently he worked as a postdoctoral fellow at the University of British Columbia, Vancouver, and at the Ecole Polytechnique Fédérale de Lausanne. In 2007, he joined the Technical University of Munich where he was a fellow of the TUM Institute for Advanced Study. He presently holds an ERC consolidator grant and a Heisenberg professorship position.

Johannes V. Barth is a Chair in Experimental Physics and Dean at the Physik-Department, TU München. His present research interests are mainly in molecular nanoscience and surface chemical physics. He holds a physics degree from Ludwig-Maximilians-Universität München and conducted his PhD studies in Physical Chemistry at the Fritz-Haber-Institut der Max-Planck-Gesellschaft, Berlin. He was a postdoctoral fellow at IBM Almaden Research Center and Fritz-Haber-Institut, Team Leader, Docent and Visiting Professor at Ecole Polytechnique Fédérale de Lausanne, and nominated a Canada Research Chair at The University of British Columbia, Vancouver, before joining the Faculty of TU München in 2007.

ACKNOWLEDGMENTS

We appreciate financial support by the EU (projects ERC Advanced Grant MolArt (no. 247299), EC FP7-PEOPLE-2011-COFUND AMAROUT II program), the TUM-HKUST Sponsorship Scheme for Targeted Strategic Partnerships, the Spanish Ministerio de Economía y

Competitividad (MINECO) (RYC-2012-11133, FIS 2013-40667-P, FIS 2015-67287-P), the Comunidad de Madrid (project MAD2D), the IMDEA Foundation, and the Munich-Center for Advanced Photonics (MAP). WA acknowledges a Heisenberg professorship by the German research foundation.

REFERENCES

(1) Eliseeva, S. V.; Bünzli, J.-C. G. Rare Earths: Jewels for Functional Materials of the Future. *New J. Chem.* **2011**, *35*, 1165-1176.
(2) Bunzli, J.-C. G.; Piguet, C. Taking Advantage of Luminescent Lanthanide Ions. *Chem. Soc. Rev.* **2005**, *34*, 1048-1077.
(3) Bünzli, J.-C. G. Review: Lanthanide Coordination Chemistry: From Old Concepts to Coordination Polymers. *J. Coord. Chem.* **2014**, *67*, 3706-3733.
(4) Pagis, C.; Ferbinteanu, M.; Rothenberg, G.; Tanase, S. Lanthanide-Based Metal Organic Frameworks: Synthetic Strategies and Catalytic Applications. *ACS Catal.* **2016**, *6*, 6063-6072.
(5) Woodruff, D. N.; Winpenny, R. E. P.; Layfield, R. A. Lanthanide Single-Molecule Magnets. *Chem. Rev.* **2013**, *113*, 5110-5148.
(6) Sessoli, R.; Powell, A. K. Strategies Towards Single Molecule Magnets Based on Lanthanide Ions. *Coord. Chem. Rev.* **2009**, *253*, 2328-2341.
(7) Gaita-Arino, A.; Prima-Garcia, H.; Cardona-Serra, S.; Escalera-Moreno, L.; Rosaleny, L. E.; Baldovi, J. J. Coherence and Organisation in Lanthanoid Complexes: From Single Ion Magnets to Spin Qubits. *Inorg. Chem. Front.* **2016**, *3*, 568-577.
(8) Thiele, S.; Balestro, F.; Ballou, R.; Klyatskaya, S.; Ruben, M.; Wernsdorfer, W. Electrically Driven Nuclear Spin Resonance in Single-Molecule Magnets. *Science* **2014**, *344*, 1135.
(9) Barth, J. V.; Costantini, G.; Kern, K. Engineering Atomic and Molecular Nanostructures at Surfaces. *Nature* **2005**, *437*, 671-679.
(10) Lin, N.; Stepanow, S.; Ruben, M.; Barth, J. V. Surface-Confined Supramolecular Coordination Chemistry. *Top. Curr. Chem.* **2009**, *287*, 1-44.
(11) Seitsonen, A. P.; Lingenfelder, M.; Spillmann, H.; Dmitriev, A.; Stepanow, S.; Lin, N.; Kern, K.; Barth, J. V. Density Functional Theory Analysis of Carboxylate-Bridged Diiron Units in Two-Dimensional Metal-Organic Grids. *J. Am. Chem. Soc.* **2006**, *126*, 5634-5635.
(12) Auwärter, W.; Ecija, D.; Klappenberger, F.; Barth, J. V. Porphyrins at Interfaces. *Nat. Chem.* **2015**, *7*, 105-120.
(13) Dong, L.; Gao, Z. A.; Lin, N. Self-Assembly of Metal-Organic Coordination Structures on Surfaces. *Prog. Surf. Sci.* **2016**, *91*, 101-135.
(14) Silly, F.; Pivetta, M.; Ternes, M.; Patthey, F.; Pelz, J. P.; Schneider, W.-D. Creation of an Atomic Superlattice by Immersing Metallic Adatoms in a Two-Dimensional Electron Sea. *Phys. Rev. Lett.* **2004**, *92*, 016101.
(15) Ormaza, M.; Fernández, L.; Ilyn, M.; Magaña, A.; Xu, B.; Verstraete, M. J.; Gastaldo, M.; Valbuena, M. A.; Gargiani, P.; Mugarza, A.; Ayuela, A.; Vitali, L.; Blanco-Rey, M.;

Schiller, F.; Ortega, J. E. High Temperature Ferromagnetism in a Gdag2 Monolayer. *Nano Lett*. **2016**, *16*, 4230-4235.
(16) Donati, F.; Rusponi, S.; Stepanow, S.; Wäckerlin, C.; Singha, A.; Persichetti, L.; Baltic, R.; Diller, K.; Patthey, F.; Fernandes, E.; Dreiser, J.; Šljivančanin, Ž.; Kummer, K.; Nistor, C.; Gambardella, P.; Brune, H. Magnetic Remanence in Single Atoms. *Science* **2016**, *352*, 318-321.
(17) Natterer, F. D.; Yang, K.; Paul, W.; Willke, P.; Choi, T.; Greber, T.; Heinrich, A. J.; Lutz, C. P. Reading and Writing Single-Atom Magnets. *Nature* **2017**, *543*, 226-228.
(18) Domingo, N.; Bellido, E.; Ruiz-Molina, D. Advances on Structuring, Integration and Magnetic Characterization of Molecular Nanomagnets on Surfaces and Devices. *Chem. Soc. Rev*. **2012**, *41*, 258-302.
(19) Cornia, A.; Mannini, M.; Sainctavit, P.; Sessoli, R. Chemical Strategies and Characterization Tools for the Organization of Single Molecule Magnets on Surfaces. *Chem. Soc. Rev*. **2011**, *40*, 3076-3091.
(20) Komeda, T.; Katoh, K.; Yamashita, M. Double-Decker Phthalocyanine Complex: Scanning Tunneling Microscopy Study of Film Formation and Spin Properties. *Prog. Surf. Sci*. **2014**, *89*, 127-160.
(21) Schlickum, U.; Decker, R.; Klappenberger, F.; Zopellaro, G.; Klyatskaya, S.; Ruben, M.; Silanes, I.; Arnau, A.; Kern, K.; Brune, H.; Barth, J. V. Metal-Organic Honeycomb Nanomeshes with Tunable Cavity Size. *Nano Lett*. **2007**, *7*, 3813-3817.
(22) Marschall, M.; Reichert, J.; Weber-Bargioni, A.; Seufert, K.; Auwärter, W.; Klyatskaya, S.; Zoppellaro, G.; Ruben, M.; Barth, J. V. Random Two-Dimensional String Networks Based on Divergent Coordination Assembly *Nat. Chem*. **2010**, *2*, 131-137.
(23) Cui, Y.; Chen, B.; Qian, G. Lanthanide Metal-Organic Frameworks for Luminescent Sensing and Light-Emitting Applications. *Coord. Chem. Rev*. **2014**, *273*, 76-86.
(24) Zhao, H.; Bazile, J. M. J.; Galán-Mascarós, J. R.; Dunbar, K. R. A Rare-Earth Metal Tcnq Magnet: Synthesis, Structure, and Magnetic Properties of $\{[Gd_2(TCNQ)_3(H_2O)_9][Gd(TCNQ)_4(H_2O)_3]\}4H_2O$. *Angew. Chem. Int. Ed*. **2003**, *42*, 1015-1018.
(25) Ballesteros-Rivas, M.; Zhao, H.; Prosvirin, A.; Reinheimer, E. W.; Toscano, R. A.; Valdés-Martínez, J.; Dunbar, K. R. Magnetic Ordering in Self-Assembled Materials Consisting of Cerium(Iii) Ions and the Radical Forms of 2,5-$TCNQX_2$ (X=Cl, Br). *Angew. Chem. Int. Ed*. **2012**, *51*, 5124-5128.
(26) Écija, D.; Urgel, J. I.; Papageorgiou, A. C.; Joshi, S.; Auwärter, W.; Seitsonen, A. P.; Klyatskaya, S.; Ruben, M.; Fischer, S.; Vijayaraghavan, S.; Reichert, J.; Barth, J. V. Five-Vertex Archimedean Surface Tessellation by Lanthanide-Directed Molecular Self-Assembly. *Proc. Natl. Acad. Sci. USA*. **2013**, *110*, 6678-6681.
(27) Urgel, J. I.; Ecija, D.; Auwärter, W.; Papageorgiou, A. C.; Seitsonen, A. P.; Vijayaraghavan, S.; Joshi, S.; Fischer, S.; Reichert, J.; Barth, J. V. Five-Vertex Lanthanide Coordination on Surfaces: A Route to Sophisticated Nanoarchitectures and Tessellations. *J. Phys. Chem. C* **2014**, *118*, 12908-12915.
(28) Chen, Z.; Klyatskaya, S.; Urgel, J. I.; Écija, D.; Fuhr, O.; Auwärter, W.; Barth, J. V.; Ruben, M. Synthesis, Characterization, Monolayer Assembly and 2d Lanthanide Coordination of a Linear Terphenyl-Di(Propiolonitrile) Linker on Ag(111). *Beilstein J. Nanotechnol*. **2015**, *6*, 327-335.

(29) Lyu, G.; Zhang, Q.; Urgel, J. I.; Kuang, G.; Auwärter, W.; Ecija, D.; Barth, J. V.; Lin, N. Tunable Lanthanide-Directed Metallosupramolecular Networks by Exploiting Coordinative Flexibility through Ligand Stoichiometry. *Chem. Commun.* **2016**, *52*, 1618-1621.
(30) Urgel, J. I.; Écija, D.; Lyu, G.; Zhang, R.; Palma, C.-A.; Auwärter, W.; Lin, N.; Barth, J. V. Quasicrystallinity Expressed in Two-Dimensional Coordination Networks. *Nat. Chem.* **2016**, *8*, 657-662.
(31) Leung, P. W.; Henley, C. L.; Chester, G. V. Dodecagonal Order in a Two-Dimensional Lennard-Jones System. *Phys. Rev. B* **1989**, *39*, 446-458.
(32) Widom, M. Bethe Ansatz Solution of the Square-Triangle Random Tiling Model. *Phys. Rev. Lett.* **1993**, *70*, 2094-2097.
(33) Ishimasa, T. Dodecagonal Quasicrystals Still in Progress. *Isr. J. Chem.* **2011**, *51*, 1216-1225.
(34) Grimm, U.; Ecija, D.; Baake, M. A Guide for Lifting Aperiodic Structures. *Zeitschrift für Kristallographie* **2016**, *231*, 507-515.
(35) Urgel, J. I.; Ecija, D.; Auwärter, W.; Stassen, D.; Bonifazi, D.; Barth, J. V. Orthogonal Insertion of Lanthanide and Transition-Metal Atoms in Metal–Organic Networks on Surfaces. *Angew. Chem. Int. Ed.* **2015**, *54*, 6163-6167.
(36) Eliseeva, S. V.; Bunzli, J.-C. G. Lanthanide Luminescence for Functional Materials and Bio-Sciences. *Chem. Soc. Rev.* **2010**, *39*, 189-227.
(37) Tanase, S.; Reedijk, J. Chemistry and Magnetism of Cyanido-Bridged D–F Assemblies. *Coord. Chem. Rev.* **2006**, *250*, 2501-2510.
(38) Huang, Y.; Jiang, F.; Hong, M. Magnetic Lanthanide–Transition-Metal Organic–Inorganic Hybrid Materials: From Discrete Clusters to Extended Frameworks. *Coord. Chem. Rev.* **2009**, *253*, 2814-2834.
(39) Ishikawa, N.; Sugita, M.; Ishikawa, T.; Koshihara, S.; Kaizu, Y. Lanthanide Double-Decker Complexes Functioning as Magnets at the Single-Molecular Level. *J. Am. Chem. Soc.* **2003**, *125*, 8694-8695.
(40) Komeda, T.; Isshiki, H.; Liu, J.; Zhang, Y.-F.; Lorente, N.; Katoh, K.; Breedlove, B. K.; Yamashita, M. Observation and Electric Current Control of a Local Spin in a Single-Molecule Magnet. *Nat. Commun.* **2011**, *2*, 217.
(41) Wäckerlin, C.; Donati, F.; Singha, A.; Baltic, R.; Rusponi, S.; Diller, K.; Patthey, F.; Pivetta, M.; Lan, Y.; Klyatskaya, S.; Ruben, M.; Brune, H.; Dreiser, J. Giant Hysteresis of Single-Molecule Magnets Adsorbed on a Nonmagnetic Insulator. *Adv. Mater.* **2016**, *28*, 5195-5199.
(42) Weber-Bargioni, A.; Reichert, J.; Seitsonen, A. P.; Auwärter, W.; Schiffrin, A.; Barth, J. V. Interaction of Cerium Atoms with Surface-Anchored Porphyrin Molecules. *J. Phys. Chem. C* **2008**, *112*, 3453-3455.
(43) Bischoff, F., TU München, 2017.
(44) Bischoff, F.; Seufert, K.; Auwärter, W.; Heim, D.; Barth, J. V. Observation of a Reaction Intermediate During the Tip-Induced Metalation of 2H-TPP with Cerium Atoms on Ag(111). *J Phys Chem C* **2017**, *Submitted*.
(45) Vijayaraghavan, S.; Auwärter, W.; Ecija, D.; Seufert, K.; Rusponi, S.; Houwaart, T.; Sautet, P.; Bocquet, M.-L.; Thakur, P.; Stepanow, S.; Schlickum, U.; Etzkorn, M.; Brune, H.; Barth, J. V. Restoring the Co Magnetic Moments at Interfacial Co-Porphyrin Arrays by Site-Selective Uptake of Iron. *ACS Nano* **2015**, *9*, 3605-3616.
(46) Nardi, M.; Verucchi, R.; Tubino, R.; Iannotta, S. Activation and Control of Organolanthanide Synthesis by Supersonic Molecular Beams: Erbium-Porphyrin Test Case. *Phys. Rev. B* **2009**, *79*, 125404.

(47) Écija, D.; Auwärter, W.; Vijayaraghavan, S.; Seufert, K.; Bischoff, F.; Tashiro, K.; Barth, J. V. Assembly and Manipulation of Rotatable Cerium Porphyrinato Sandwich Complexes on a Surface. *Angew. Chem. Int. Ed.* **2011**, *50*, 3872-3877.
(48) Vijayaraghavan, S.; Écija, D.; Auwärter, W.; Joshi, S.; Seufert, K.; Seitsonen, A. P.; Tashiro, K.; Barth, J. V. Selective Supramolecular Fullerene–Porphyrin Interactions and Switching in Surface-Confined C60–Ce(TPP)$_2$ Dyads. *Nano Lett.* **2012**, *12*, 4077-4083.
(49) Furukawa, H.; Cordova, K. E.; O'Keeffe, M.; Yaghi, O. M. The Chemistry and Applications of Metal-Organic Frameworks. *Science* **2013**, *341*.
(50) Pagis, C.; Ferbinteanu, M.; Rothenberg, G.; Tanase, S. Lanthanide-Based Metal Organic Frameworks: Synthetic Strategies and Catalytic Applications. *ACS Catalysis* **2016**, *6*, 6063-6072.
(51) Barth, J. V. Molecular Architectonic on Metal Surfaces. *Annu. Rev. Phys. Chem.* **2007**, *58*, 375-407.
(52) Urgel, J. I.; Cirera, B.; Wang, Y.; Auwärter, W.; Otero, R.; Gallego, J. M.; Alcamí, M.; Klyatskaya, S.; Ruben, M.; Martin, F.; Miranda, R.; Ecija, D.; Barth, J. V. Surface-Supported Robust Two-Dimensional Lanthanide-Carboxylate Coordination Networks. *Small* **2015**, *47*, 6358-6364.
(53) Cirera, B.; Dordevic, L.; Otero, R.; Gallego, J. M.; Bonifazi, D.; Miranda, R.; Ecija, D. Dysprosium-Carboxylate Nanomeshes with Tunable Cavity Size and Assembly Motif through Ionic Interactions. *Chem. Commun.* **2016**, *52*, 11227-11230.
(54) Urgel, J. I.; Ecija, D.; Auwärter, W.; Barth, J. V. Controlled Manipulation of Gadolinium Coordinated Supramolecules by Low-Temperature Scanning Tunneling Microscopy. *Nano Lett.* **2014**, *14*, 1369.